Available online at www.sciencedirect.com
SCIENCE DIRECT®
International Journal of Heat and Mass Transfer 48 (2005) 2323–2332
International Journal of HEAT and MASS TRANSFER
www.elsevier.com/locate/ijhmt

Free convective mass transfer at circular thin disk electrodes with varying inclination

J. Krýsa [a], W. Reuter [b,1], A.A. Wragg [b,*]

[a] Department of Inorganic Technology, Institute of Chemical Technology, Technicka 5, l66 28 Prague 6, Czech Republic
[b] Department of Engineering, University of Exeter, North Park Road, Exeter EX4 4QF, UK

Received 11 August 2004
Available online 17 March 2005

Abstract

The electrochemical limiting diffusion current technique was used to evaluate free convective mass transfer rates at free-standing circular disk electrodes of varying inclination and diameter. The electrochemical system used was copper deposition from acidified cupric sulphate solution. Experiments were carried with the single faces active and also with both faces simultaneously active. A Toepler–Schlieren system was used to photovisualise the ascending convection streams in order to obtain flow pattern information. For the upward-facing surface, the flow separates at a certain distance from the leading edge of the inclined disk, whereas the flow on the downward-facing surface always stays attached. The data correlations for the doubled disks show an exponent in the *Sh*–*Ra* correlation ranging from 0.25 (vertical case), indicating laminar flow, to 0.294 (horizontal case), indicating a mixed effect of turbulent separated flow on the upward-facing side and attached flow on the downward-facing surface. A universal correlation $Sh_d = f_A(Ra_d)^{f_B}$ was obtained for disk diameters d from 5 to 80 mm and inclination angle from 0° to 90° (from the vertical) where f_A and f_B are functions of inclination.

1. Introduction

The fundamental equations for free convection heat transfer include the well-known laws of continuity of matter, momentum and energy in a fluid. Many references present the development of these equations; for example Welty et al. [1] or Burmeister [2], while Jaluria [3] performs a derivation of these equations with the aim of describing natural convective flows.

The application of these equations to practical problems of free convective heat transfer and their solutions has been performed only for simple geometries (isothermal or uniformly heated vertical or horizontal plates). However, solutions for complex geometries or more complex fluid flow phenomena, such as boundary layer characteristics, instability and separated flow, remains a very difficult task. Therefore experimental data and empirical correlations are widely used to evaluate practical free convective transfer problems.

Mass transfer measurements are known to provide good simulation of free convective heat transfer [4]. The electrochemical limiting diffusion current technique of mass transfer measurement is attractive as a modelling method for heat transfer since the measurements

* Corresponding author. Tel.: +44 1392 263656; fax: +44 1392 217965.
E-mail address: a.a.wragg@ex.ac.uk (A.A. Wragg).
[1] Present address: BMW AG, 80788 Munich, Germany.

0017-9310/$ - see front matter © 2005 Elsevier Ltd. All rights reserved.
doi:10.1016/j.ijheatmasstransfer.2005.01.006

Nomenclature

A	coefficient in correlating Eq. (4)
B	exponent in correlating Eq. (4)
c_b	bulk concentration of Cu^{2+} ions, mol m^{-3}
D	diffusion coefficient of Cu^{2+} ions, m^2 s^{-1}
d	diameter of disk, m
F	Faraday constant, 96487 C mol^{-1}
g	gravitational acceleration, 9.81 m s^{-2}
Gr_d	Grashof number based on disk diameter d, Eq. (2)
I_L	limiting diffusion current, A
k	mass transfer coefficient, m s^{-1}, Eq. (1)
n	charge number of Cu^{2+} ion (=2)
Ra_d	Rayleigh number based on disk diameter d, Eq. (2)
S	surface area, m^2
Sc	Schmidt number, Eq. (2)
Sh_d	Sherwood number based on disk diameter d, Eq. (3)
T	electrolyte temperature, K
μ	dynamic viscosity, kg m^{-1} s^{-1}
θ	inclination angle from vertical, deg or °
$\Delta\rho$	density difference between bulk solution and interface, kg m^{-3}
ρ	density of bulk solution, kg m^{-3}

are usually simpler, cheaper and speedier than direct heat transfer measurements. Moreover, it is also easy to determine the heat transfer performance of the individual surfaces in a complex multi-surface geometry by isolating unwanted surfaces. An example of the use of the electrochemical technique as a low temperature modelling method for the simulation of passive heat loss from cuboid shaped electronic components is found in [5]. Apart from the heat transfer simulation free convection mass transfer data is also important in technical applications such as electroplating, etching, electro reforming and electropolishing.

There are many geometries for which considerable heat transfer data exists. Among geometries that have received the most attention in studies of natural convection in external flow fields are vertical flat surfaces [6–8] and horizontal surfaces in both down-facing [6,9,10] and up-facing orientation [6,7,11]. Another often studied geometry is the inclined surface [12–14]. A geometry which is only rarely reported is that of a thin free-standing circular disk. Kobus et al. studied free convective heat transfer to vertical [15] and horizontal disks [16]. Data from inclined thin disks appear to be absent from the free convective heat (mass) literature. Therefore the present work deals with free convective mass transfer at free standing (double sided) disks of various inclinations. A further advantage of the electrochemical technique, additional to those already mentioned above, is that we can measure mass transfer at both single surfaces and their combination which is experimentally impossible for heat transfer. The aim of this study was:

(a) to measure mass transfer rates at either a single face or both faces of thin disks of varying diameter and inclination;
(b) to visualise the flow around such inclined disks;
(c) to obtain a universal correlation of data for various disk diameter and inclination for the purpose of prediction of heat transfer rate.

2. Experimental

The experiments were performed in a rectangular 3 dm^3 optical glass sided container of dimensions 15×30 cm and height 25 cm. The technique used involved the cathodic deposition of cupric ions from a $CuSO_4/H_2SO_4/H_2O$ electrolyte. In order to vary the density difference between bulk fluid and surface the cupric ion concentration was varied from 0.01 to 0.21 mol dm^{-3}. Each solution contained 1.5 mol dm^{-3} sulphuric acid as supporting electrolyte. The actual Cu^{2+} concentration was periodically determined by spectrophotometric analysis.

The disk cathodes were made from thin copper sheet or foil. The diameters varied from 80 mm to 5 mm. The thickness was chosen to be as small as possible so as to reduce side surface effects but big enough to enable the handling described below. The wire for holding and electrically connecting the disk was soldered onto an edge of the disk and carefully insulated. The disks manufactured and used in the experiments are listed in Table 1. The insulation of the wire connection was achieved using a lacquer (Lacomit). For the experiments with single sided disks one side of the disks and also the side surface were also carefully lacquered. The counter electrode (anode)

Table 1
Geometric details of electrodes

Disk diameter d (mm)	Disk thickness (mm)	Wire thickness (mm)	Ratio of side area to total area (%)
80	1.25	2.0	3.0
60	1.25	1.5	4.0
40	0.50	1.2	2.4
20	0.25	1.0	2.4
10	0.25	0.8	4.7
5	0.25	0.5	9.1

was a cylindrical copper mesh of diameter 18 cm and height 23 cm placed partially around the sides of the tank. The arrangement of the apparatus is similar to that described previously [17]. For the setting of an inclination angle the supporting mechanism, shown in Fig. 1 was used. For the flow visualisation the disk cathodes were placed in the center of the container, in the field of view of a standard Toepler–Schlieren optical system with a camera [18,19] (Fig. 2).

The usual electrical circuit (Fig. 2) for limiting current measurement was employed, consisting of a dc power supply with a voltage regulator, a high impedance voltmeter and a multi-range ammeter. Limiting currents were obtained by the well known procedure, which has been reported in detail previously [20]. The anode acted as a reference electrode in view of its high area compared to that of the cathode. Under such conditions polarisation is negligible at the anode and the cell current–voltage relationship depends predominantly on the conditions prevailing at the cathode. The onset of the limiting current was sharp and reproducible. In some experiments current transients were recorded by suddenly applying a potential corresponding to the limiting plateau region. As soon as convection was visible Schlieren photographs were taken at various stages of flow development and the limiting current was simultaneously recorded.

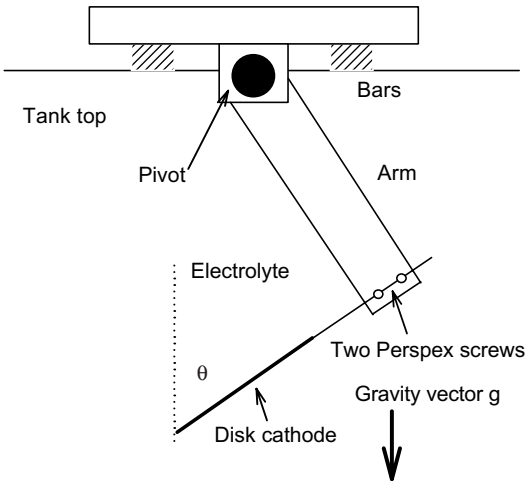

Fig. 1. Electrode support mechanism.

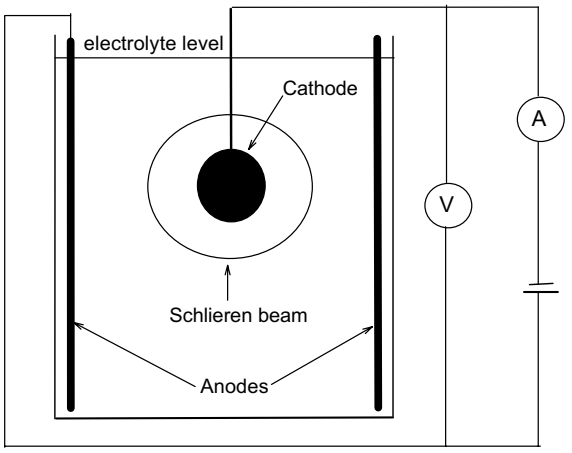

Fig. 2. Electrode arrangement and electrical circuit.

3. Results

3.1. Mass transfer data calculation

For each experiment the mass transfer coefficient was calculated from the measured limiting current using the equation:

$$k = \frac{I_L}{SnFc_b} \tag{1}$$

The area in this equation was the total available for mass transfer for the particular experiment.

For the disk surfaces the diameter was used as characteristic dimension in the Sherwood and Rayleigh numbers

$$Ra_d = Gr_d Sc = \frac{g\Delta\rho d^3\rho}{\mu^2}\frac{\mu}{\rho D} = \frac{g\Delta\rho d^3}{\mu D} \tag{2}$$

$$Sh_d = \frac{kd}{D} \tag{3}$$

For a single inclination the correlation equation was used in the form

$$Sh_d = A\mathrm{Ra}_d^B \tag{4}$$

The diffusivity of the Cu^{2+} ions was calculated using the data of Wilke et al. [21]. Electrolyte density and viscosity were calculated using data of Eisenberg et al. [22]. The $\Delta\rho$ terms were taken from Wilke et al. [21]. The effect of migration on the copper deposition rate was negligible (see [23]).

3.2. Effect of inclination on mass transfer data

The effect of inclination on k for single sided disks of diameter 10 mm and 60 mm and with cupric sulphate concentration 0.12 M is shown in Fig. 3. Both graphs have similar features. It is obvious that the downward-facing surface shows a totally different behaviour than the upward-facing one. k increases strongly starting from $\theta = -90°$ (horizontal downfacing), which produces the smallest value of k. The increase $dk/d\theta$ becomes

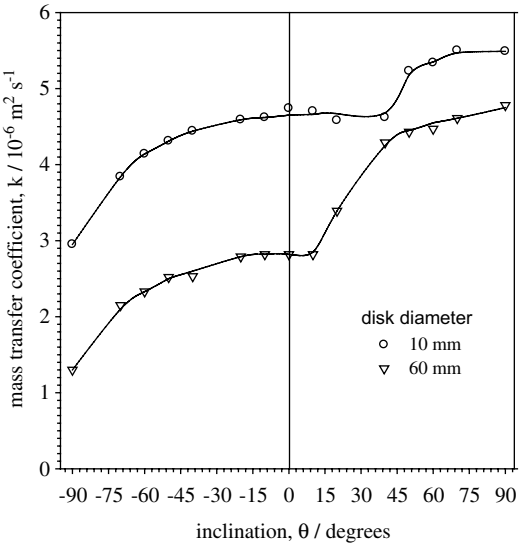

Fig. 3. The effect of inclination on mass transfer coefficient for single disks of diameter 10 mm and 60 mm in cupric sulphate concentration of 0.12 M.

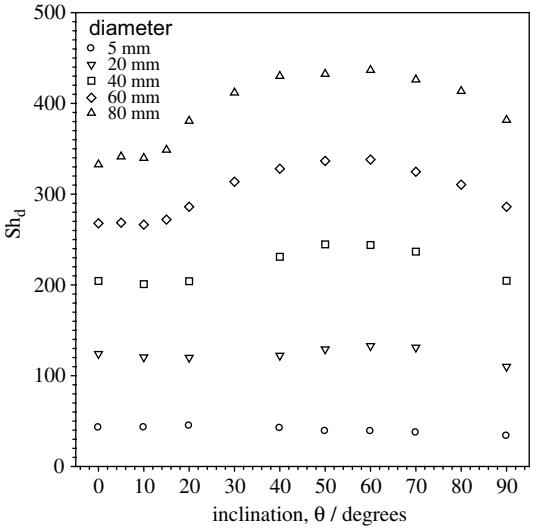

Fig. 4. The effect of inclination on *Sh* for double sided disk of various diameter in single cupric sulphate concentration of 0.12 M.

smaller as the vertical position is approached and seems to reach zero there. In the region of small angle variations from the vertical (±10°), only small changes in mass transfer coefficient are observed. With increasing inclination from the vertical for the upward-facing surface k stays approximately constant until a certain inclination θ_1 is reached. From this point there is a strong increase in k towards a maximum value for the horizontal upward-facing surface at $\theta = +90°$. The gradient $dk/d\theta$, which is at its biggest value for θ_1, decreases continuously towards $\theta = +90°$. One striking difference in the curves is the angle θ_1, at which the upper surface changes its mass transfer behaviour sharply. For the smaller disk $d = 10$ mm this angle is about $\theta_1 = 40°$, while for the big disk $d = 60$ mm it is about $\theta_1 = 10°$. Otherwise the shape of both curves is similar. It is worth noting that the 60 mm disk gives four times higher mass transfer in the up-facing horizontal orientation (+90°) compared to down-facing. The comparison of single sided disk data (for diameter 60 mm) with Eq. (6) in [24] was performed for all inclinations. We found an average deviation of about 8% which can be explained by the fact that Quaraishi and Fahidy [24] used inter-electrode distance as characteristic length in the *Ra* and *Sh* numbers.

The effect of inclination on the Sherwood number for double sided disks for several diameters and a single concentration of cupric sulphate of 0.12 M is shown in Fig. 4. The *Sh* versus θ plots show very characteristic behaviour for the different disk sizes. Direct comparison of the vertical and horizontal positions show that for small *Ra* numbers (small disks) *Sh* for the vertical position is higher. This overall tendency changes with equal values at horizontal and vertical positions for the 40 mm disk in $c = 0.12$ M solution. For large *Ra* numbers (disks with $d = 60$ and 80 mm at $c = 0.12$ M in Fig. 4) *Sh* for the horizontal position is higher. Thus for 'small' disks the vertical position has better mass transfer than the horizontal while for 'big' disks the opposite is true. The four larger disks also show a local maximum in the region of about $\theta = 60°$ and the overall shape of the plots is similar. For the smallest disks $d = 5$ and 10 mm (not shown) no maximum is visible, instead a slight overall monotonic decrease occurs from $\theta = 0°$ to 90.

It is instructive to compare results from single sided disks with the corresponding data from the same disks in the same solution with both sides active. *Sh* for the single up-facing surface, the single down-facing surface and the double sided (both faces active) disks are plotted against inclination for $d = 60$ mm and $c = 0.12$ M in Fig. 5. For a direct comparison of the mass transfer results, the average *Sh* number for the two single sides averaged is also calculated and plotted. This value of *Sh* is the result for the two active surfaces without any interaction or error due to disk thickness. Comparison of the double-sided results with the average of the single-sided results was also performed for a disk size of 10 mm and both cases lead to the same conclusion. This shows that the average *Sh* of the single active sides is higher than that for both sides simultaneously active and that an almost constant difference between the two exists. For $d = 10$ mm *Sh* for the double sided disk lies about 14%

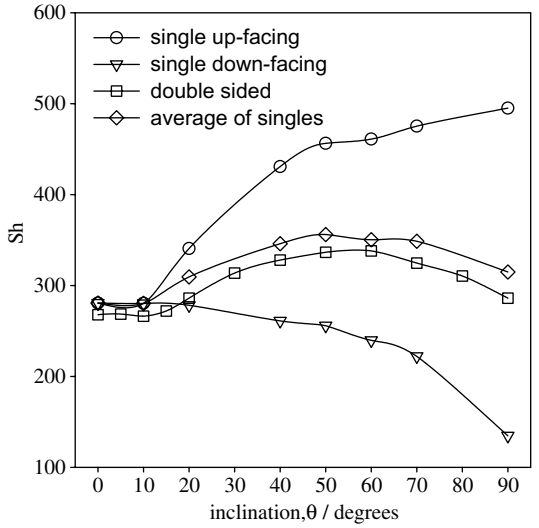

Fig. 5. Comparison of the *Sh* number dependence on inclination for various surfaces and combinations of surfaces, disk of diameter 60 mm.

below the average of the single sides. For the disk $d = 60$ mm this mean difference is about 6%. The constant difference in *Sh* numbers implies an effect or a mixture of effects for the double sided disks that is consistent for all inclinations. These effects are due to interaction between the two main surfaces and the existence of a side surface in the experiments with double sided disks.

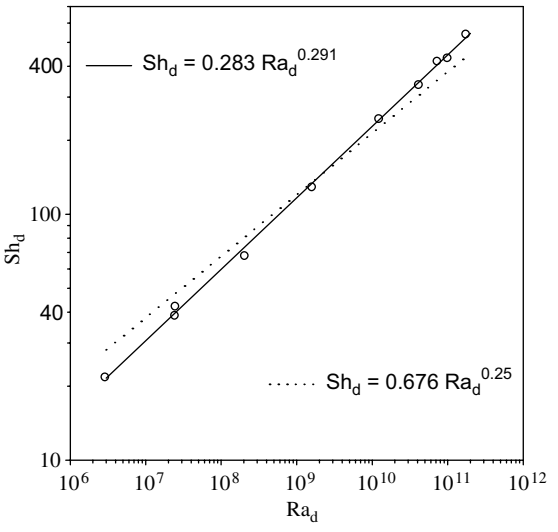

Fig. 6. Mass transfer correlation for double sided disks at inclination 50°.

3.3. Mass transfer correlation for double sided disks

It was observed that data for one inclination gives a good correlation when plotted as $\log Sh$ versus $\log Ra$ (Eq. (4)), as shown in Fig. 6 for inclination $\theta = 50°$. The least squares fit through the data gives the correlating equation.

$$Sh_d = 0.283 Ra_d^{0.291} \quad (5)$$

For comparison a line with a forced slope of $b = 0.25$ is also shown as a broken line which corresponds to the relationship

$$Sh_d = 0.676 Ra_d^{0.25} \quad (6)$$

The results of least squares analysis of all data from double sided disks at various inclinations are shown in Table 2. The mass transfer data correlated well for all inclinations with values of the correlation coefficient within $0.9995 \leqslant R^2 \geqslant 0.9975$. Correlation with a forced exponent $B = 0.25$ was also determined for each inclination. However, these correlations were not able to include the lower or higher *Sh*/*Ra* number pairs of data adequately especially for the higher inclinations $\theta \geqslant 40°$. The possible explanation is that for inclination angles around 40° separation of flow occurs and flow becomes turbulent. Similar behaviour (for inclined plates) was observed in our previous work [25]. Separation of flow depends on the inclined length as well as angle of inclination; e.g. for shorter inclined lengths separation will occur at higher inclinations. In the following attempt to obtain a universal correlation, including the inclination effect, the forced power correlations were not further investigated.

The exponent obtained for vertical disks (0.25) shows that an attached laminar boundary layer exists on both sides. The behaviour changes as inclination increases as pointed out by several authors [25,26,24]. Tritton [27] showed for inclined plates that inclination has a stabilising effect on the flow below the disk and a destabilising one for flow above the disk. Thus the boundary layer below the disk always remains attached and shows laminar

Table 2
Coefficients *A* and exponents *B* (Eq. (4)) for various inclinations of double sided disks

θ/°	*A*	*B*
0	0.622	0.250
10	0.540	0.256
20	0.498	0.262
40	0.369	0.279
50	0.283	0.291
60	0.288	0.290
70	0.286	0.289
90	0.227	0.294

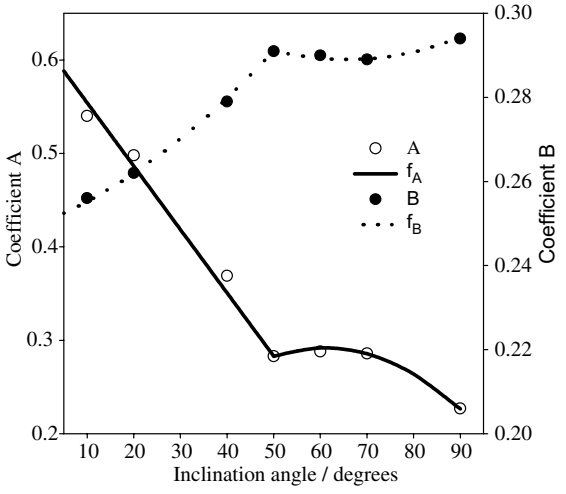

Fig. 7. Dependence of correlating coefficient A and power B on inclination angle.

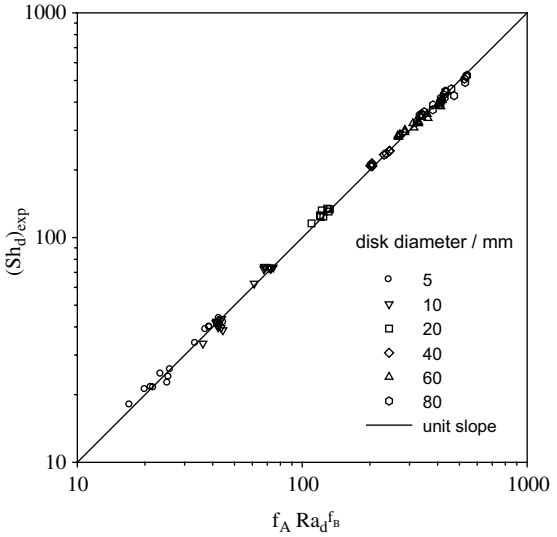

Fig. 8. Universal mass transfer correlation for double sided disks.

behaviour, as for the vertical surfaces. The boundary layer on the upward/inclined surface, however, separates at a certain length up the disk, depending on inclination, and becomes turbulent, as also observed by Patrick and Wragg [28] for inclined rectangular surfaces.

For all double sided disks with large inclination from the vertical the mass transfer measured consists of two separate contributions by the two surfaces which behave very differently. Therefore attempts to include the inclination effect on mass transfer correlations by inserting a factor of $\cos\theta$, as in many publications on single-sided plates [25,26,12,13], does not produce a satisfactory solution for double sided disks. This approach can be used only for down-facing inclined surfaces.

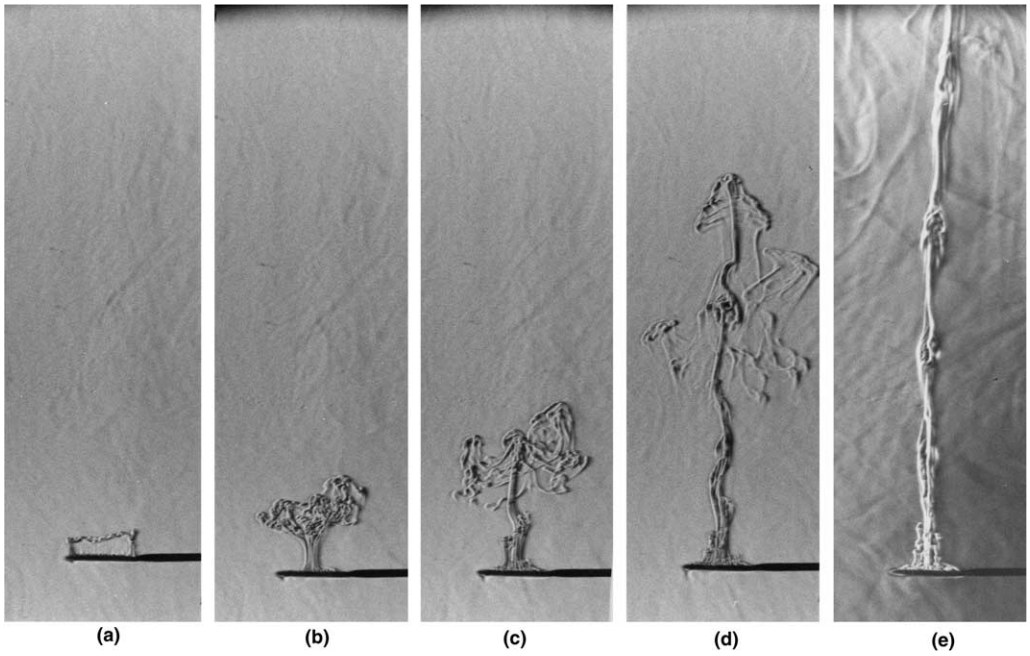

Fig. 9. Flow development at double sided disk of 10 mm diameter in the horizontal position, 90° (in 0.19 mol dm^{-3} cupric sulphate): (a) 3 s after potential switch-on, (b) 7 s, (c) 12 s, (d) 30 s, (e) in steady state.

In order to correlate the experimental data for all inclination angles, θ, in one single equation, the correlating coefficients A and B shown in Table 2 were further analysed and a general correlation for double sided disks of various inclinations is proposed

$$Sh_d = f_A(Ra_d)^{f_B} \tag{7}$$

where f_A and f_B are functions of inclination angle. The coefficient A is plotted versus inclination angle in Fig. 7. The values of A over the range $0° \leqslant \theta \geqslant 90$ can be approximated by two analytical functions valid for two separate regions of inclination. The division is made at $\theta = 50°$, where the behaviour for f_A changes significantly.

$$f_A = 0.622 - \frac{0.339}{50}\theta \quad \text{for } \theta \leqslant 50° \tag{8a}$$

and

$$f_A = 0.292 - 7.75 \times 10^{-5}(\theta - 60.97)^2 \quad \text{for } \theta \geqslant 50° \tag{8b}$$

The coefficient B is also plotted versus inclination angle in Fig. 7. The range of inclinations is conveniently divided into two regions again at $\theta = 50$. Two different second order functions were used to approximate the behaviour for f_B giving

$$f_B = 0.243 + 7.33 \times 10^{-6}(\theta + 30.91)^2 \quad \text{for } \theta \leqslant 50° \tag{9a}$$

and

$$f_B = 0.289 - 8.75 \times 10^{-6}(\theta - 65.71)^2 \quad \text{for } \theta \geqslant 50° \tag{9b}$$

The quality of the universal correlation was tested by comparing calculated Sherwood numbers (Eq. (7)) with experimentally found Sherwood numbers for each disk and inclination angle in Fig. 8. A line with unit slope represents a perfect match of experiment and calculation. The experimental data differs from the calculation with a maximum of 9% and has an average difference of 3.5%. It is thus possible to use Eq. (7) with f_A and f_B by Eqs. (8) and (9) for the prediction of mass (heat) transfer rate at double sided disks of any inclination with good accuracy.

3.4. Flow observation

Fig. 9 shows a transient series after potential switch-on for a horizontal double sided disk of $d = 10$ mm. In Fig. 9a shortly after potential is applied the first liquid layer depleted in cupric ions rises in a ring at the outer periphery. The rise of fluid from the upper surface creates a pressure gradient towards the center of the disk which pulls the flow inwards (see Fig. 9b) in a laminar boundary layer flow. The fluid from the very start of the process has risen further and creates a mushroom shape with a well defined single laminar plume following. In Fig. 9c a turbulent 'burst' from the upper surface can be observed, where the boundary layer flow collapses and separates closer to the outer edge, and then rises in a turbulent thicker plume (Fig. 9d). It can be observed that the flow around the electrode is of pulsing nature with turbulent bursts of liquid from the upper surface and laminar boundary flow from the down-facing surface which causes an oscillation in the mass transfer rate and the limiting current. The pulsing occurs at a constant frequency, shown by the almost equally spaced rising knots of turbulent fluid (see Fig. 9e).

The disk of 5 mm diameter also shows a pulsing behaviour with an overall stronger laminar flow and equally spaced bursts of turbulent fluid (see Fig. 10a). Fig. 10b displays a totally laminar flow at an inclination of $\theta = 50°$. In comparison to the horizontal position (Fig. 10a) the flow is not pulsing. It stays attached on the upper surface, as well as the lower, and separates from the 'trailing edge' in a laminar fashion.

Fig. 11 shows the flow around a double sided disk of diameter 40 mm at different inclination angles of 90°, 70° and 50°. A three-dimensional multi-columnar flow

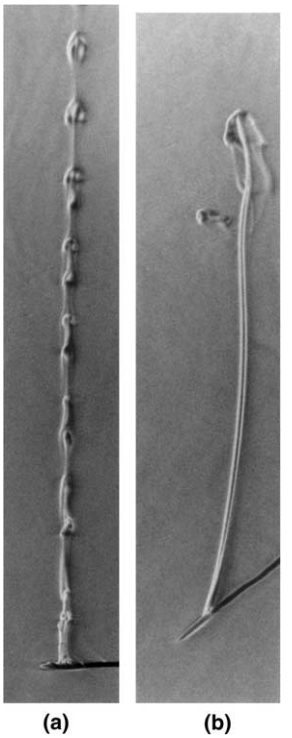

Fig. 10. Steady state flow patterns for double sided disk of 5 mm diameter at different inclinations: (a) 90° and (b) 50° (in 0.19 mol dm^{-3} cupric sulphate).

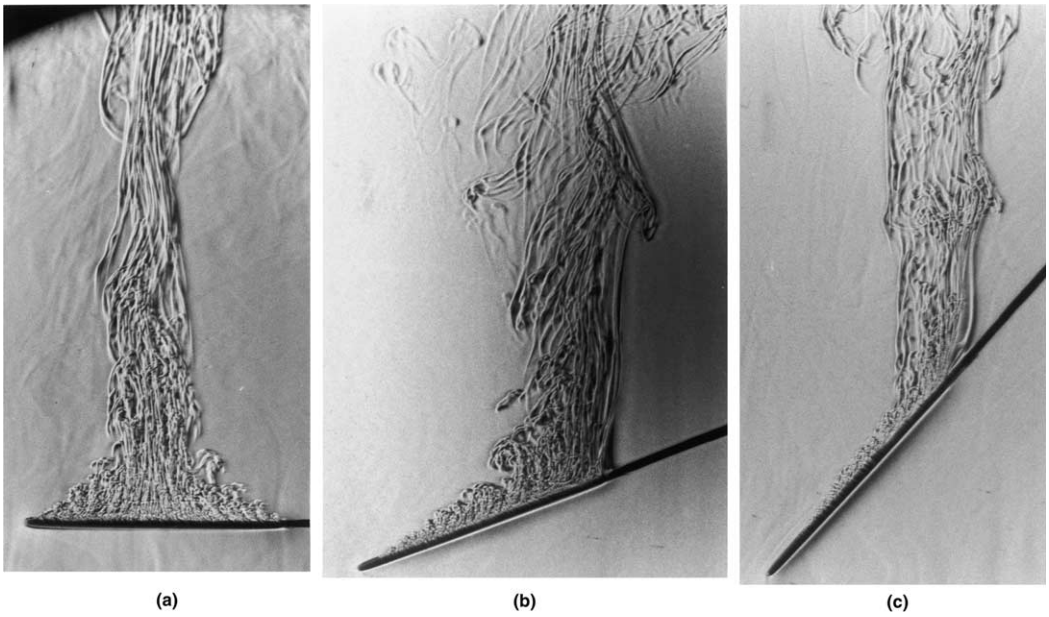

Fig. 11. Steady state flow patterns for double sided disk of 40 mm diameter at different inclinations: (a) 90°, (b)70° and (c) 50° (in 0.19 mol dm^{-3} cupric sulphate).

can be observed above the horizontal disk (Fig. 11a) with separation near the outer edge. At $\theta = 70°$ (Fig. 11b) the flow is no longer axi-symmetric but shows a short laminar boundary layer region near the leading

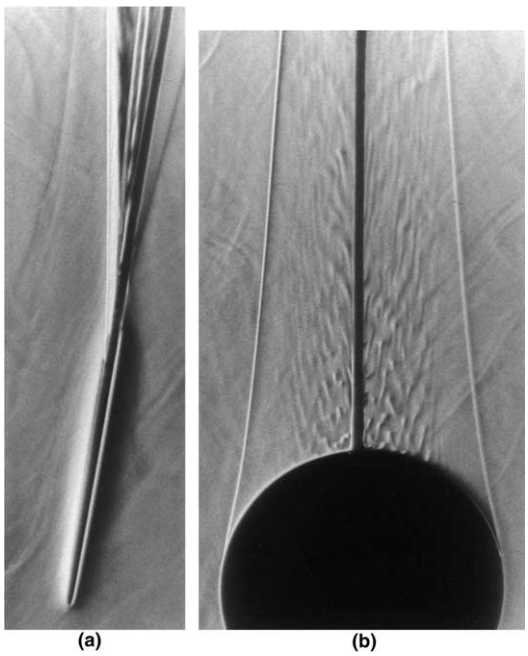

Fig. 12. Photographs of steady state flow at a double disk of 40 mm diameter at 10°: (a) light beam parallel to the surface, (b) light beam normal to the surface.

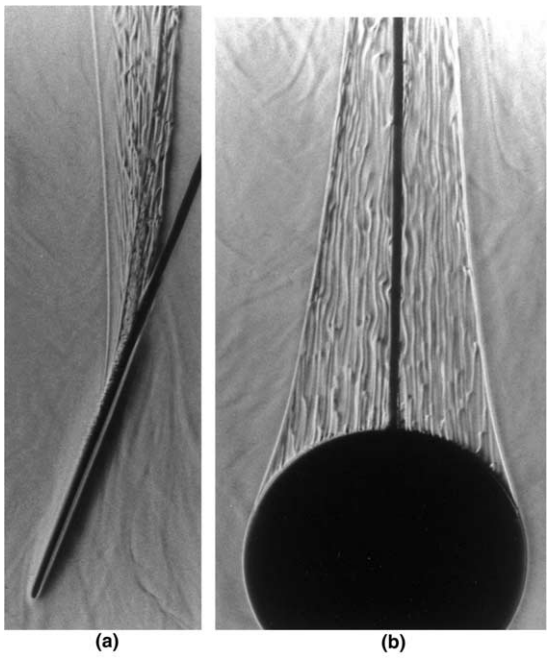

Fig. 13. Photographs of steady state flow at a double disk of 40 mm diameter at 20°: (a) light beam parallel to the surface, (b) light beam normal to the surface.

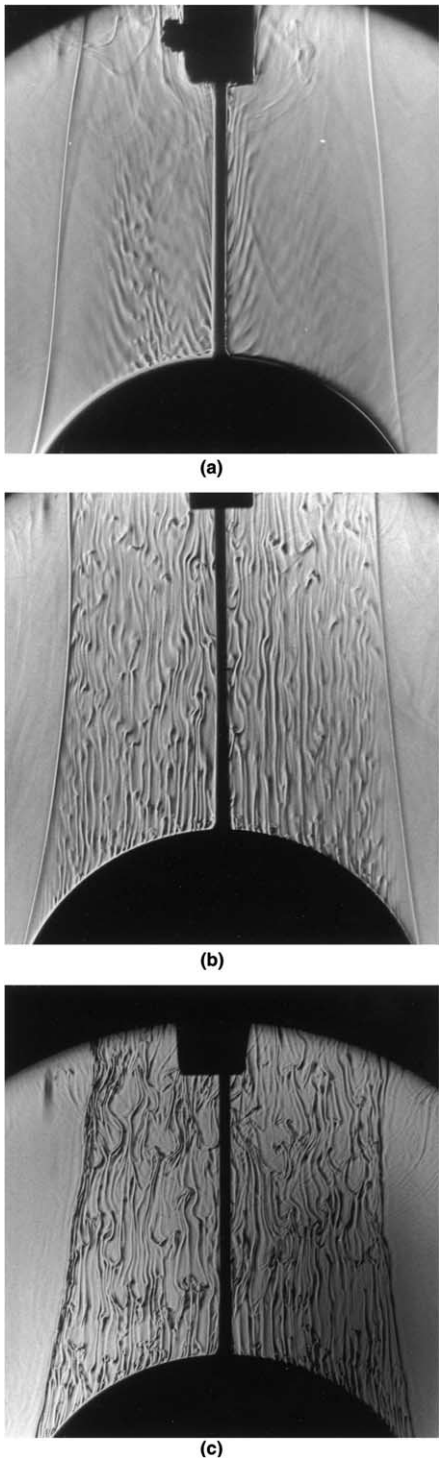

Fig. 14. Photographs of steady state flow at a double disk of 80 mm diameter with light beam normal to the surface: (a) at 0°, (b) at 10°, (c) at 20°.

edge. It separates further up the surface to rise in a similar multi-columnar plume. The flow at $\theta = 50°$ (Fig. 11b) shows a longer region of attached boundary layer flow on the upper surface that becomes turbulent and separates further up the disk. The rising plume is still multi-columnar and three-dimensional. Laminar flow on the underside is also visible at all inclinations.

Fig. 12a shows the flow around a disk of $d = 40$ at $\theta = 10°$ with a laminar boundary layer on the upper surface staying attached until the trailing edge. The Schlieren picture normal to the plume (Fig. 12b) detects wavelike instability patterns in the flow rising from the disk. Fig. 13a with the same disk at $\theta = 20°$ displays some turbulent structure in the boundary layer flow on the upper surface. Nevertheless it stays attached up to the trailing edge and the normal view shows stronger instability patterns (Fig. 13b) giving evidence of longitudinal vortices.

The photographs in Fig. 14 were all taken normal to the disk and show the flow rising from a disk of $d = 80$ mm at $\theta = 0°$, 10° and 20°. The complex flow rising from the trailing edge shows increasing strength of the vertical striations (vortex structure) with increasing angle.

4. Conclusions

Disks with only one side active were investigated to highlight the effect of side interaction between the two surfaces of inclined disks. Mass transfer shows a minimum in the downward-facing horizontal position, a monotonic rise towards the vertical position with almost no change in mass transfer for small inclinations from the vertical, and a maximum in the upward-facing horizontal position. For the upward-facing surface an angle can be identified at which a strong rise in mass transfer occurs, and which is dependent on disk size. This marks the beginning of a different flow regime on the upper surface.

Due to the interaction of the flow from the two surfaces, the double sided disks have Sh values lower than the average Sh of the two single sides. The mass transfer data for double sided disks were correlated for each inclination angle θ, using the disk diameter as characteristic length. Approximating functions f_A and f_B were used to express the dependence of coefficient A and power B on inclination. Thus a universal correlation was produced $Sh_d = f_A(Ra_d)^{f_B}$ with the power f_B varying from 0.25 (vertical case) to 0.294 (horizontal case).

The flow on the lower surface stays attached for all inclinations, while the flow along the upper surface becomes turbulent and separated. Wave type instabilities in the rising plume can be identified at small angles of inclination from the vertical and longitudinal vortices at larger inclinations.

Acknowledgments

This research was partially supported by the Ministry of Education, Youth and Sports of the Czech Republic (project number CEZ: MSM 223100001 and 6046137301). WR's visit to Exeter was made possible trough the Erasmus student exchange programme.

References

[1] J.R. Welty, C.E. Wicks, R.E. Wilson, Fundam. Momentum, Heat Mass Transfer, John Wiley & Sons, New York, 1969.
[2] L.C. Burmeister, Convective Heat Transfer, John Wiley & Sons, New York, 1983.
[3] Y. Jaluria, Natural Convection Heat and Mass Transfer, HMT The Series & Application of Heat and Mass Transfer, vol. 5, Pergamon Press, Oxford, 1980.
[4] M.A. Patrick, A.A. Wragg, Modelling of free convection heat transfer using electrochemical mass transfer techniques, I. Chem. Eng. Symp. Ser. 94 (1985) 45–55.
[5] D.R.E. Worthington, M.A. Patrick, A.A. Wragg, Effect of shape on natural convection heat and mass transfer at horizontally oriented cuboids, Chem. Eng. Res. Des. 65 (1987) 131–137.
[6] A.-J.N. Khalifa, Natural convective heat transfer coefficient a review I. Isolated vertical and horizontal surfaces, Energy Convers. Manage. 42 (2001) 491–504.
[7] V.V. Vlassov, G.A. Dreitser, Experimental investigation of natural convective heat transfer from a round plate of complex configuration, Int. J. Heat Mass Transfer 44 (2001) 755–767.
[8] G. Maranza, S. Didierjean, B. Rémy, D. Maillet, Experimental estimation of the transient free convection heat transfer coefficient on a vertical flat plate in air, Int. J. Heat Mass Transfer 45 (2002) 3413–3427.
[9] A. Dayan, R. Kushnir, A. Ullmann, Laminar free convection underneath a hot horizontal infinite flat strip, Int. J. Heat Mass Transfer 45 (2002) 4021–4031.
[10] E. Radziemska, W.M. Lewandovski, Heat transfer by natural convection from a isothermal downward-facing round plate in unlimited space, Appl. Energy 68 (2001) 347–366.
[11] W.M. Lewandovski, E. Radziemska, M. Buzuk, H. Bieszk, Free convection heat transfer and fluid flow above horizontal rectangular plates, Appl. Energy 66 (2000) 177–197.
[12] N. Onur, M.K. Aktas, An experimental study on the effect of opposing wall on natural convection along an inclined hot plate facing downward, Int. Commun. Heat Mass Transfer 25 (1998) 389–397.
[13] J. Khedari, P. Yimsamerjit, J. Hirunlabh, Experimental investigation of free convection in a roof solar collector, Build. Environ. 37 (2002) 455–459.
[14] H.X. Yang, Z.J. Zhu, Numerical study on transient laminar natural convection in a parallel-walled channel, Int. Commun. Heat Mass Transfer 30 (2003) 359–367.
[15] C.J. Kobus, G.L. Wedekind, An experimental investigation into forced, natural and combined forced and natural convective heat transfer from stationary isothermal circular disks, Int. J. Heat Mass Transfer 38 (1995) 3329–3339.
[16] C.J. Kobus, G.L. Wedekind, An experimental investigation into natural convective heat transfer from horizontal isothermal circular disks, Int. J. Heat Mass Transfer 44 (2001) 3381–3384.
[17] J. Krýsa, F. Iino, A.A. Wragg, Free convective mass transfer at down-pointing isosceles triangles of varying inclination, Collect. Czech. Chem. Commun. 63 (1998) 2114–2122.
[18] D.W. Holder, R.J. North, Schlieren Methods, Notes on Applied Science, No. 31, National Physical Laboratory, London, 1963.
[19] M. Jakob, Heat Transfer, vol. I, Wiley, 1949, Chapter 27.
[20] A.F.J. Smith, A.A. Wragg, An electrochemical study of mass transfer in free convection at vertical arrays of horizontal cylinders, J. Appl. Electrochem. 4 (1974) 219–228.
[21] C.R. Wilke, C.W. Tobias, M. Eisenberg, Correlation of limiting currents under free convective condition, J. Electrochem. Soc. 100 (1953) 513–517.
[22] M. Eisenberg, C.W. Tobias, C.R. Wilke, Selected properties of ternary electrolytes employed in ionic mass transfer studies, J. Electrochem. Soc. 103 (1956) 413–416.
[23] N. Ibl, O. Dossenbach, in: E. Yeager, J.O'. M. Bockris, B.E. Conway, S. Sarangapani (Eds.), Comprehensive Treatise of Electrochemistry, vol. 6, Plenum Press, New York, 1983, pp. 192–198.
[24] M.S. Quaraishi, T.Z. Fahidy, Free-convective ionic mass transport at inclined circular disk electrodes, Electrochim. Acta 23 (1978) 33–38.
[25] M.A. Patrick, A.A. Wragg, D.M. Pargeter, Mass transfer by free convection during electrolysis at inclined electrodes, Can. J. Chem. Eng. 55 (1977) 432–438.
[26] J.R. Lloyd, E.M. Sparrow, E.R.G. Eckert, Local natural convection mass transfer measurements, J. Electrochem. Soc. 119 (1972) 702–707.
[27] D.J. Tritton, Transition to turbulence in the free convection boundary layers on an inclined heated plate, J. Fluid Mech. 16 (1963) 417–435.
[28] M.A. Patrick, A.A. Wragg, Steady and transient natural convection at inclined planes and cones, Phys. Chem. Hydrodyn. 5 (1984) 299–306.